derived from the known structures of closely related compounds.[4,5] The structure of Ib, which has been discussed extensively in the earlier calculational work,[23] was used as the "standard" geometry. That is, all hydrogen arrangements investigated were examined with this fixed cluster core geometry. However, as the Fe–B distance in this model was 2.21 Å, several calculations were carried out with the non-hydrogen-bridged Fe–B edges set at 2.00 Å. As there were no large differences in the results and as the shorter Fe–B distances distorted the cluster, not all structures were investigated in this fashion. The basis functions and exponents used in the calculations were the same as used previously.[23]

**Acknowledgment.** The support of the National Science Foundation under Grant CHE 84-08251 is gratefully acknowledged. We also thank the Notre Dame Computing Center for computing time and the donors of the Petroleum Research Fund, administered by the American Chemical Society, for support of this research.

**Registry No.** Ia, 67517-57-1; II·$Ph_4As$, 110796-05-9; II·$(C_2H_5)_3NH$, 110796-07-1; II·PPN, 110796-08-2; III, 80572-82-3; IV, 108008-76-0; $[BH_2Fe_3(CO)_{10}]^-$, 92078-18-7; $Fe(CO)_5$, 13463-40-6; $Fe_2(CO)_9$, 15321-51-4.

**Supplementary Material Available:** Text, one table, and one figure summarizing pertinent results of Fenske–Hall calculations (3 pages). Ordering information is given on any current masthead page.

---

Contribution from the Department of Chemistry and Laboratory for Molecular Structure and Bonding,
Texas A&M University, College Station, Texas 77843

# Further Study of Metal–Metal Bond Lengths in Homologous Edge-Sharing Bioctahedral Complexes

Jo Ann M. Canich, F. Albert Cotton,* Lee M. Daniels, and Diane B. Lewis

*Received May 19, 1987*

Four new compounds have been prepared and characterized structurally: $Mo_2Cl_6(dmpm)_2$ (**1**), $W_2Cl_6(dmpm)_2$ (**2**), $W_2Cl_6(dppm)_2$ (**3**), and $Re_2Cl_6(dmpm)_2$ (**4**) (where dmpm = $Me_2PCH_2PMe_2$ and dppm = $Ph_2PCH_2PPh_2$). The structural data for these four compounds combined with similar data previously published[1] for five other homologous compounds provide a more detailed and secure picture of how M–M bonding in edge-sharing bioctahedral complexes depends on the number of d electrons available. The previous conclusion that in molecules of the type studied here, i.e., $M_2Cl_6(dRpm)_2$, the M–M bonding orbitals are filled in the order $\sigma$, $\pi$, $\delta^*$, $\delta$, $\pi^*$, $\sigma^*$ is validated. However, the row (second or third transition series) from which the metal atom originates and the choice of diphosphine ligand (dmpm or dppm) are found to be factors of greater importance than was previously recognized. Crystallographic data for the new compounds as well as their M–M distances are as follows: **1**, $P2_1/n$ with $a$ = 6.976 (2) Å, $b$ = 15.559 (6) Å, $c$ = 11.000 (6) Å, $\beta$ = 94.24 (3)°, and $Z$ = 2, Mo–Mo = 2.7394 (5) Å; **2**, $P2_1/c$ with $a$ = 8.625 (2) Å, $b$ = 20.229 (3) Å, $c$ = 8.676 (2) Å, $\beta$ = 92.80 (2)°, and $Z$ = 2, W–W = 2.6663 (4) Å; **3**, $C2/c$ with $a$ = 23.025 (9) Å, $b$ = 10.938 (4) Å, $c$ = 21.722 (9) Å, $\beta$ = 117.61 (3)°, and $Z$ = 4, W–W = 2.691 (1) Å; **4**, $P2_1/n$ with $a$ = 6.9140 (6) Å, $b$ = 15.358 (1) Å, $c$ = 10.8621 (9) Å, $\beta$ = 94.894 (7)°, and $Z$ = 2, Re–Re = 2.5807 (4) Å.

## Introduction

Several years ago we reported structural results[1] on a series of compounds of type I, from which certain conclusions were drawn as to the ordering of the $\sigma$, $\pi$, $\delta$, $\delta^*$, $\pi^*$, and $\sigma^*$ orbitals that are primarily involved in the M–M interaction. It was stressed in the discussion of that work that if M to M distances in edge-sharing bioctahedral complexes[2] are to be used as an index of the strength of the M–M bonding it is important to maintain all factors other than the number of electrons available to fill such orbitals as nearly invariant as possible. Such factors as the oxidation state of the metal, the size of the metal atoms, and the identity of the ligands are crucial. In the series of five compounds presented in that earlier study we were forced to compromise slightly on this requirement. In particular, we included complexes formed by both second- and third-transition-series elements and used both $(CH_3)_2PCH_2P(CH_3)_2$ (dmpm) and $(C_6H_5)_2PCH_2P(C_6H_5)_2$ (dppm) ligands because of our inability to synthesize a series of compounds confined entirely to one transition series and to one of the two diphosphine ligands. We suggested that, because of the well-known effect of the lanthanide contraction, the employment of both second- and third-row metal atoms would not have a serious effect and supported this with data for analogous Nb and Ta complexes where the M–M distances differed only slightly compared to the differences from one bond order to another. As for the changes from dmpm to dppm, we had no control experiment but assumed that this would also be only a tolerably minor perturbation.

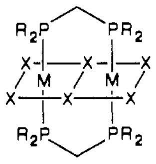

I: R = $CH_3$, $C_6H_5$; X = Cl

We have now been able to prepare and structurally characterize four more compounds of type I. These provide direct tests of both of the previous assumptions. They show (a) that the assumptions were less satisfactory than we had believed but (b) that the main conclusion as to the ordering of the molecular orbitals is still valid. The four new compounds and their identifying numbers that will be used throughout are $Mo_2Cl_6(dmpm)_2$ (**1**), $W_2Cl_6(dmpm)_2$ (**2**), $W_2Cl_6(dppm)_2$ (**3**), and $Re_2Cl_6(dmpm)_2$ (**4**).

## Experimental Section

All manipulations were carried out under an atmosphere of argon by using standard Schlenk and vacuum line techniques. Commercial-grade solvents were purchased from Fischer Scientific Co. Toluene and hexane were distilled from benzophenone ketyl prior to use, while $CH_2Cl_2$ was dried by distillation from phosphorus pentoxide. Bis(dimethylphosphino)methane (dppm) was purchased from Organometallics, Inc., and chlorine gas was obtained from Matheson Gas Products, Inc. The infrared and visible spectra were recorded on Perkin-Elmer 783 and Cary 17D spectrophotometers, respectively.

**Preparation of Crystalline Compounds. Compound 1.** The starting material, $Mo_2Cl_4(dmpm)_2$, was prepared by a literature method.[3] A 0.25-g amount of $Mo_2Cl_4(dmpm)_2$ dissolved in 25 mL of $CH_2Cl_2$ was placed in a test tube, which was then fitted with a septum. Chlorine gas was introduced through the septum via a disposable pipet for 45–90 s. During this time the solution changed from blue to bright orange, and the solvent was immediately removed under vacuum. The product was recrystallized by slow evaporation of a $CH_2Cl_2$ solution (yield 83%).

**Compound 2.** The starting material, $W_2Cl_4[P(n\text{-}Bu)_3]_4$, was prepared by a literature method.[4] To a 100-mL round-bottom flask equipped with

---

[1] Chakravarty, A. R.; Cotton, F. A.; Diebold, M. P.; Lewis, D. B.; Roth, W. J. *J. Am. Chem. Soc.* **1986**, *108*, 971.

[2] Cotton, F. A. *Polyhedron* **1987**, *6*, 667.

[3] Cotton, F. A.; Falvello, L. R.; Harwood, W. S.; Powell, G. L.; Walton, R. A. *Inorg. Chem.* **1986**, *25*, 3949.

0020-1669/87/1326-4046$01.50/0

**Table I.** Crystal Data for Compounds **1–4**

| | **1** | **2** | **3** | **4** |
|---|---|---|---|---|
| formula | $Mo_2Cl_6P_4C_{10}H_{28}$ | $W_2Cl_{10}P_4C_{12}H_{32}$ | $W_2Cl_6P_4C_{50}H_{44}$ | $Re_2Cl_6P_4C_{10}H_{28}$ |
| fw | 676.82 | 1022.5 | 1349.22 | 857.36 |
| space group | $P2_1/n$ | $P2_1/c$ | $C2/c$ | $P2_1/n$ |
| systematic absences | $0k0$, $k \neq 2n$; $h0l$, $h + l \neq 2n$ | $h0l$, $l \neq 2n$; $0k0$, $k \neq 2n$ | $hkl$, $h + k \neq 2n$; $h0l$, $l \neq 2n$ | $0k0$, $k \neq 2n$; $h0l$, $h + l \neq 2n$ |
| $a$, Å | 6.976 (2) | 8.625 (2) | 23.025 (9) | 6.9140 (6) |
| $b$, Å | 15.559 (6) | 20.229 (3) | 10.938 (4) | 15.358 (1) |
| $c$, Å | 11.000 (6) | 8.676 (2) | 21.722 (9) | 10.8621 (9) |
| $\beta$, deg | 94.24 (3) | 92.80 (2) | 117.61 (3) | 94.894 (7) |
| $V$, Å$^3$ | 1191 (1) | 1512 (1) | 4848 (4) | |
| $Z$ | 2 | 2 | 4 | 2 |
| $d_{calcd}$, g/cm$^3$ | 1.887 | 2.246 | 1.850 | 2.478 |
| cryst size, mm | 0.2 × 0.2 × 0.3 | 0.3 × 0.2 × 0.1 | 0.2 × 0.2 × 0.05 | 0.2 × 0.2 × 0.4 |
| $\mu$(Mo K$\alpha$), cm$^{-1}$ | 19.57 | 88.759 | 53.497 | 116.46 |
| data collecn instrument | Syntex $P\bar{1}$ | Enraf-Nonius CAD-4S | Enraf-Nonius CAD-4S | Rigaku AFC5 |
| radiation (monochromated in incident beam) | Mo K$\alpha$ ($\lambda_{\bar{\alpha}}$ = 0.71073 Å) | Mo K$\alpha$ ($\lambda_{\bar{\alpha}}$ = 0.71073 Å) | Mo K$\alpha$ ($\lambda_{\bar{\alpha}}$ = 0.71073 Å) | Mo K$\alpha$ ($\lambda_{\bar{\alpha}}$ = 0.71073 Å) |
| orientation rflns: no.; range ($2\theta$), deg | 25; 18–30 | 25; 16.2–35.4 | 25; 13.0–34.5 | 25; 18–30 |
| temp, °C | 20 | 22 | 20 | 19 |
| scan method | $\omega$–$2\theta$ | $\omega$ | $\omega$–$2\theta$ | $\omega$–$2\theta$ |
| data colecn range, $2\theta$, deg | 4–55 | 2–45 | 4–45 | 4–50 |
| no. of unique data, total with $F_o^2 > 3\sigma(F_o^2)$ | 2438<br>2389 | 2650<br>1970 | 3166<br>1886 | 1682 |
| no. of params refined | 100 | 135 | 280 | 100 |
| transmission factors: max; min | 100; 0.82 | 0.9996; 0.6408 | 0.9993; 0.7365 | 0.628; 1.000 |
| $R^a$ | 0.0355 | 0.02745 | 0.03587 | 0.0291 |
| $R_w{}^b$ | 0.0587 | 0.03588 | 0.04308 | 0.0459 |
| quality-of-fit indicator$^c$ | 1.432 | 1.020 | 1.063 | 1.071 |
| large shift/esd, final cycle | 0.01 | 0.00 | 0.01 | 0.02 |
| largest peak, e/Å | 1.17 | 1.226 | 0.774 | 1.18 |

[a] $R = \sum||F_o| - |F_c||/\sum|F_o|$. [b] $R_w = [\sum w(|F_o| - |F_c|)^2/\sum w|F_o|^2]^{1/2}$; $w = 1/\sigma^2(|F_o|)$. [c] Quality of fit $= [\sum w(|F_o| - |F_c|)^2/(N_{observns} - N_{params})]^{1/2}$.

a side arm and reflux condenser were added 0.50 g (0.38 mmol) of $W_2Cl_4[P(n\text{-Bu})_3]_4$, 0.13 mL of dmpm (0.834 mmol), 10 mL of toluene, and 20 mL of hexane. The mixture was stirred and refluxed for 4 h, after which a dark semicrystalline material precipitated out. The solution was decanted from the solid, leaving behind a mixture of red and green solids. The green solid, presumably $W_2Cl_4(dmpm)_2$ on the basis of absorption bands at 452 and 668 nm, was separated from the red solid by dissolving the mixture in 15 mL of toluene and filtering off the insoluble red substance. To this solution was added 10 mL of $CH_2Cl_2$ as the oxidizing agent. The solution was filtered into a Schlenk flask and layered with 10 mL of hexane. Over a period of several weeks, small green-yellow crystals formed, which were characterized as $W_2Cl_6(dmpm)_2$ by X-ray diffraction. No effort was made to optimize the yield.

**Compound 3.** The starting material, $W_2Cl_4(dppm)_2$, was prepared by a literature procedure.[5] Two preparative methods for **3** were employed; in method 1, the oxidizing agent was $Cl_2$, while in method 2, the solvent $CH_2Cl_2$ served as the oxidizing agent.

**Method 1.** In a 100-mL round-bottom Schlenk flask, 0.10 g (0.078 mmol) of $W_2Cl_4(dppm)_2$ was dissolved in 20 mL of $CH_2Cl_2$. Chlorine gas (1.8 mL, at 1 atm, 0.075 mmol) was syringed into the solution, and the mixture was stirred for 1 h, during which time the brown solution became slightly lighter in color. The solvent was vacuum-transferred to a trap at −196 °C and left behind a yellow-brown solid identified as $W_2Cl_6(dppm)_2$ from its characteristic visible spectrum.[6] IR (Nujol, CsI; cm$^{-1}$): 1587 (w), 1574 (w), 1486 (m), 1436 (s), 1310 (w), 1263 (w), 1191 (w), 1165 (w), 1124 (w), 1097 (m), 1074 (w), 1030 (w), 1002 (w), 975 (vw), 923 (vw), 894 (vw), 848 (vw), 784 (s), 754 (m), 739 (s), 727 (s), 704 (m), 692 (s), 623 (w), 618 (w), 529 (ms), 512 (m), 483 (m), 458 (w), 430 (w), 403 (vw), 358 (vw), 347 (w), 330 (vw), 314 (m), 300 (vw), 295 (w), 280 (w). Visible ($CH_2Cl_2$; nm): 465 (s), 384 (s).

**Method 2.** The compound $W_2Cl_4(dppm)_2$ (0.05 g, 0.04 mmol) was dissolved in 20 mL of $CH_2Cl_2$ in a 100-mL round-bottom Schlenk flask. After 2.5 h, the reaction was monitored by visible spectroscopy, which showed absorption bands from both the product, $W_2Cl_6(dppm)_2$, and the reactant, $W_2Cl_4(dppm)_2$, in the spectrum. After 21 h, approximately 95% of the $W_2Cl_4(dppm)_2$ had been converted to product; after 92 h, the reaction was complete. The solvent was removed via dynamic vacuum to a trap held at −196 °C, leaving behind $W_2Cl_6(dppm)_2$ in near-quantitative yield.

**Crystallization of Compound 3.** Several attempts were made to grow X-ray crystallographic quality crystals by layering $CH_2Cl_2$ solutions of $W_2Cl_6(dppm)_2$ with hexane or by placing concentrated $CH_2Cl_2$ solutions in a refrigerator at 0 °C. The latter method produced large dark green block-shaped crystals that were so highly susceptible to solvent loss that they could not be handled outside of the mother liquor. Attempts to mount these crystals were unsuccessful. The crystals used for X-ray data collection were produced as a side product of another reaction. When 0.10 g (0.078 mmol) of $W_2Cl_4(dppm)_2$ and 0.0191 g (0.087 mmol) of PhSSPh were dissolved in 20 mL of $CH_2Cl_2$ and refluxed for 0.5 h, a brown solution was generated. This solution was filtered, transferred to a Schlenk tube, and layered with 10 mL of hexane. Small green-yellow crystals of $W_2Cl_6(dppm)_2$ were produced among crystals of $W_2(SPh)Cl_5(dppm)_2$.

**Compound 4.** A solution of 0.25 g (0.219 mmol) of $(n\text{-Bu}_4N)_2Re_2Cl_8$ in 25 mL of dry, distilled $CH_2Cl_2$ was placed in a Schlenk tube under argon. A solution containing 0.10 mL (0.70 mmol) of bis(dimethylphosphino)methane in 10 mL of acetone was carefully layered on top of the $CH_2Cl_2$ solution. Within 3 days, dark purple crystals of $Re_2Cl_6(dmpm)_2$ had formed on the sides of the tube. The supernatant liquid was transferred to another flask, where further mixing afforded precipitation of more product, total yield 0.135 g (72%).

**Crystallographic Procedures.** The general procedures used for data collection, data reduction, and the solution and refinement of the structures were those routinely used in this laboratory.[6,7] Important details pertinent to particular compounds are presented in Table I and in the following paragraphs. For all compounds, observed and calculated structure factors are available as supplementary material.

**Compound 1.** Systematic absences uniquely determined the space group as $P2_1/n$. The position of the Mo atom was located from a three-dimensional Patterson function. The rest of the non-hydrogen atoms were located and refined by an alternating sequence of least-squares cycles and difference Fourier maps. All atoms were included first with isotropic and then with anisotropic displacement parameters. Final atomic positional and isotropic-equivalent displacement parameters are listed in Table II.

**Compound 2.** Crystals of this compound are prone to lose interstitial $CH_2Cl_2$ of crystallization and had to be carefully mounted in a glass

---

(4) Schrock, R. R.; Sturgeoff, L. G.; Sharp, P. R. *Inorg. Chem.* **1983**, *22*, 2801.

(5) Canich, J. M.; Cotton, F. A. *Inorg. Chim. Acta*, in press.

(6) (a) Bino, A.; Cotton, F. A.; Fanwick, P. E. *Inorg. Chem.* **1979**, *18*, 3558. (b) Cotton, F. A.; Frenz, B. A.; Deganello, G.; Shaver, A. *J. Organomet. Chem.* **1973**, *50*, 227.

(7) Calculations were done on the VAX-11/780 computer at the Department of Chemistry, Texas A&M University, College Station, TX, with the VAX-SDP software package.

**Table II.** Atomic Positional Parameters and Equivalent Isotropic Displacement Parameters and Their Estimated Standard Deviations for $Mo_2Cl_6(\mu\text{-dmpm})_2$[a]

| atom | *x* | *y* | *z* | $B_{eq}$, Å$^2$ |
|---|---|---|---|---|
| Mo(1) | 0.05629 (4) | 0.06044 (2) | 0.08588 (3) | 1.979 (6) |
| Cl(1) | 0.2469 (1) | 0.01134 (6) | −0.07230 (8) | 2.76 (2) |
| Cl(2) | −0.0597 (2) | 0.12316 (7) | 0.2690 (1) | 4.02 (2) |
| Cl(3) | 0.3278 (2) | 0.15654 (7) | 0.1254 (1) | 3.94 (2) |
| P(1) | −0.0925 (2) | 0.18327 (6) | −0.04253 (9) | 2.50 (2) |
| P(2) | 0.2083 (2) | −0.05047 (6) | 0.23464 (9) | 2.57 (2) |
| C(1) | −0.2824 (6) | 0.1490 (3) | −0.1570 (4) | 2.91 (7) |
| C(2) | −0.2173 (8) | 0.2650 (3) | 0.0395 (5) | 4.0 (1) |
| C(3) | 0.0831 (7) | 0.2435 (3) | −0.1219 (4) | 4.10 (9) |
| C(4) | 0.4251 (8) | −0.0149 (3) | 0.3244 (4) | 4.1 (1) |
| C(5) | 0.0515 (8) | −0.0865 (4) | 0.3496 (4) | 4.4 (1) |

[a] Anisotropically refined atoms are given in the form of the equivalent isotropic displacement parameter defined as $^4/_3[a^2\beta_{11} + b^2\beta_{22} + c^2\beta_{33} + ab(\cos\gamma)\beta_{12} + ac(\cos\beta)\beta_{13} + bc(\cos\alpha)\beta_{23}]$.

**Table III.** Atomic Positional Parameters and Equivalent Isotropic Displacement Parameters and Their Estimated Standard Deviations for $W_2Cl_6(dmpm)_2{\cdot}2CH_2Cl_2$[a]

| atom | *x* | *y* | *z* | *B*, Å$^2$ |
|---|---|---|---|---|
| W(1) | 0.05642 (3) | 0.05077 (1) | 0.08312 (3) | 1.785 (5) |
| Cl(1) | 0.1607 (2) | 0.01405 (9) | −0.1516 (2) | 2.52 (4) |
| Cl(2) | −0.0088 (3) | 0.1136 (1) | 0.3114 (3) | 3.41 (4) |
| Cl(3) | 0.2746 (2) | 0.1271 (1) | 0.0761 (3) | 3.32 (4) |
| P(1) | 0.2337 (2) | −0.0211 (1) | 0.2552 (2) | 2.33 (4) |
| P(2) | −0.1142 (2) | 0.13465 (9) | −0.0587 (3) | 2.45 (4) |
| C(1) | 0.1706 (9) | −0.1080 (4) | 0.256 (1) | 3.0 (2) |
| C(2) | 0.246 (1) | −0.0005 (5) | 0.460 (1) | 3.9 (2) |
| C(3) | 0.4367 (9) | −0.0223 (5) | 0.203 (1) | 3.8 (2) |
| C(4) | −0.032 (1) | 0.2164 (4) | −0.086 (1) | 4.4 (2) |
| C(5) | −0.295 (1) | −0.1515 (5) | 0.034 (1) | 4.4 (2) |
| H(1) | 0.26 (1) | −0.137 (6) | 0.31 (1) | 3 (2)* |
| H(2) | 0.078 (9) | −0.113 (4) | 0.31 (1) | 1 (2)* |
| Cl(4) | −0.4560 (3) | 0.1725 (2) | 0.4215 (4) | 5.69 (7) |
| Cl(5) | −0.6847 (4) | 0.1731 (1) | 0.6546 (4) | 6.24 (7) |
| C(6) | 0.641 (1) | 0.1998 (5) | 0.467 (1) | 4.6 (2) |

[a] Anisotropically refined atoms are given in the form of the equivalent isotropic displacement parameter defined as $^4/_3[a^2\beta_{11} + b^2\beta_{22} + c^2\beta_{33} + ab(\cos\gamma)\beta_{12} + ac(\cos\beta)\beta_{13} + bc(\cos\alpha)\beta_{23}]$. Starred values denote atoms refined isotropically.

capillary, protected also by epoxy cement. The space group, $P2_1/c$, was uniquely determined from the systematic absences in the intensity data. The position of the unique tungsten atom was determined from the Patterson map. The remaining non-hydrogen atoms were located by a series of alternate difference Fourier and least-squares refinement cycles. The hydrogen atoms on the bridging carbon atoms were also located in this manner and were refined isotropically. All other atoms, including those from the solvent molecule, were anisotropically refined to give the final residuals. The possibility of an orthorhombic *c*-centered cell was eliminated after final refinement by testing the data for equivalent reflections. A poor agreement factor of 72% was found with the space group *Cmmm*. We can therefore conclude that the chosen monoclinic space group indeed is correct. Fractional coordinates are presented in Table III. The complete formula is $W_2Cl_6(dmpm)_2{\cdot}2CH_2Cl_2$.

**Compound 3.** The *c* diagonal was photographed to verify centering for the monoclinic cell. Systematic absences in the intensity data narrowed the choice of space groups to *C*2/*c* and *Cc*. The position of the unique tungsten atom was determined from the Patterson map, and the centrosymmetric space group was chosen and found to be correct. The remaining non-hydrogen atoms were located by successive difference Fourier maps and least-squares refinement cycles. At that point, an additional empirical absorption correction[8] was made prior to anisotropic refinement of the atoms. Location of hydrogen atoms was not pursued. Fractional coordinates are listed in Table IV.

**Table IV.** Atomic Positional Parameters and Equivalent Isotropic Displacement Parameters and Their Estimated Standard Deviations for $W_2Cl_6(dppm)_2$[a]

| atom | *x* | *y* | *z* | *B*, Å$^2$ |
|---|---|---|---|---|
| W(1) | 0.71243 (2) | 0.20004 (5) | 0.02581 (3) | 2.575 (9) |
| Cl(1) | 0.7641 (1) | 0.3972 (3) | 0.0589 (2) | 3.31 (7) |
| Cl(2) | 0.8393 (2) | 0.4941 (3) | −0.0209 (2) | 4.03 (9) |
| Cl(3) | 0.8359 (2) | 0.2406 (3) | −0.0987 (2) | 4.34 (9) |
| P(1) | 0.8107 (2) | 0.1148 (3) | 0.1337 (2) | 3.09 (8) |
| P(2) | 0.6048 (2) | 0.2728 (3) | −0.0760 (2) | 3.03 (8) |
| C(1) | 0.8850 (5) | 0.206 (1) | 0.1543 (6) | 3.2 (3) |
| C(2) | 0.8023 (6) | 0.125 (1) | 0.2135 (6) | 3.8 (3) |
| C(3) | 0.7665 (8) | 0.037 (2) | 0.2256 (8) | 7.6 (5) |
| C(4) | 0.7574 (9) | 0.044 (2) | 0.2852 (9) | 9.2 (6) |
| C(5) | 0.7826 (7) | 0.139 (2) | 0.3321 (8) | 7.0 (5) |
| C(6) | 0.8166 (8) | 0.225 (2) | 0.3195 (7) | 6.3 (5) |
| C(7) | 0.8278 (7) | 0.222 (1) | 0.2584 (7) | 5.2 (4) |
| C(8) | 0.8382 (6) | −0.042 (1) | 0.1363 (7) | 4.2 (4) |
| C(9) | 0.8097 (6) | −0.118 (1) | 0.0775 (7) | 4.2 (4) |
| C(10) | 0.8323 (7) | −0.238 (1) | 0.0835 (9) | 5.7 (5) |
| C(11) | 0.877 (1) | −0.287 (2) | 0.142 (1) | 10.0 (8) |
| C(12) | 0.906 (1) | −0.213 (2) | 0.198 (1) | 11.2 (8) |
| C(13) | 0.886 (1) | −0.086 (1) | 0.1960 (9) | 8.8 (7) |
| C(14) | 0.5640 (6) | 0.413 (1) | −0.0703 (6) | 3.7 (3) |
| C(15) | 0.5956 (6) | 0.494 (1) | −0.0183 (7) | 4.1 (3) |
| C(16) | 0.5647 (7) | 0.606 (1) | −0.0172 (7) | 5.5 (4) |
| C(17) | 0.5009 (8) | 0.630 (2) | −0.0691 (8) | 7.0 (5) |
| C(18) | 0.4688 (8) | 0.543 (2) | −0.1195 (9) | 7.9 (5) |
| C(19) | 0.4982 (7) | 0.436 (2) | −0.1207 (8) | 6.9 (5) |
| C(20) | 0.5389 (6) | 0.157 (1) | −0.1039 (7) | 4.0 (4) |
| C(21) | 0.5226 (8) | 0.082 (1) | −0.1600 (8) | 6.3 (5) |
| C(22) | 0.4700 (9) | −0.004 (2) | −0.1790 (9) | 6.9 (5) |
| C(23) | 0.4401 (7) | −0.016 (1) | −0.1387 (9) | 6.6 (5) |
| C(24) | 0.4570 (8) | 0.063 (2) | −0.0814 (9) | 8.2 (6) |
| C(25) | 0.5055 (7) | 0.147 (2) | −0.0657 (8) | 6.1 (5) |

[a] Anisotropically refined atoms are given in the form of the equivalent isotropic displacement parameter defined as $^4/_3[a^2\beta_{11} + b^2\beta_{22} + c^2\beta_{33} + ab(\cos\gamma)\beta_{12} + ac(\cos\beta)\beta_{13} + bc(\cos\alpha)\beta_{23}]$. Starred values denote atoms refined isotropically.

**Table V.** Positional and Isotropic Equivalent Thermal Parameters for $Re_2Cl_6(dmpm)_2$[a]

| atom | *x* | *y* | *z* | *B*, Å$^2$ |
|---|---|---|---|---|
| Re | 0.05254 (4) | −0.05710 (2) | 0.08337 (3) | 1.444 (6) |
| Cl(1) | 0.2542 (3) | −0.0128 (1) | −0.0707 (2) | 2.28 (4) |
| Cl(2) | −0.0630 (4) | −0.1208 (2) | 0.2661 (2) | 3.36 (5) |
| Cl(3) | 0.3224 (3) | −0.1536 (2) | 0.1326 (2) | 3.25 (5) |
| P(1) | −0.0832 (3) | −0.1799 (1) | −0.0368 (2) | 2.10 (4) |
| P(2) | 0.1991 (3) | 0.0478 (2) | 0.2318 (2) | 2.23 (4) |
| C(1) | −0.273 (1) | −0.1473 (6) | −0.1559 (8) | 2.6 (2) |
| C(2) | −0.209 (2) | −0.2628 (7) | 0.046 (1) | 3.9 (2) |
| C(3) | 0.089 (1) | −0.2432 (7) | −0.116 (1) | 4.1 (2) |
| C(4) | 0.417 (1) | 0.0114 (7) | 0.3277 (9) | 3.9 (2) |
| C(5) | 0.043 (2) | 0.0855 (8) | 0.3492 (9) | 4.1 (2) |
| H(1) | −0.3906 | −0.1368 | −0.1187 | 3.3* |
| H(2) | −0.2930 | −0.1924 | −0.2154 | 3.3* |

[a] Starred values denote atoms that were not refined but used only to calculate structure factors. Anisotropically refined atoms are given in the form of the isotropic equivalent displacement parameter defined as $^4/_3[a^2\beta_{11} + b^2\beta_{22} + c^2\beta_{33} + ab(\cos\gamma)\beta_{12} + ac(\cos\beta)\beta_{13} + bc(\cos\alpha)\beta_{23}]$.

**Compound 4.** A well-formed pinacoidal crystal was mounted on the end of a glass fiber. The crystal was shown to belong to the monoclinic system, and systematic absences unambiguously identified the space group as $P2_1/n$. The Patterson vector corresponding to the metal–metal bond was used to position the Re atom. The remaining non-hydrogen atoms appeared in a single difference Fourier synthesis based on refined parameters for the Re atom. Following full-matrix refinement of all parameters for the non-hydrogen atoms, a difference Fourier map revealed peaks corresponding to the two methylene hydrogen atoms on the bridging carbon atom. Attempted full-matrix refinement with unconstrained hydrogen atoms was unsuccessful; however, calculation of structure factors including calculated positions for the bridging hydrogen atoms did improve the discrepancy indices. Ideal hydrogen atom positions were therefore calculated with a C–H distance fixed at 0.95 Å and an isotropic temperature factor of 3.3 Å$^2$. The atomic positional parameters are listed in Table V.

## Results

All four compounds were shown to have the desired type of structure, i.e., structure I. Figure 1 is an ORTEP drawing of the

---

(8) Pauling, L. *The Nature of the Chemical Bond*, 3rd ed.; Cornell University Press: Ithaca, NY, 1960; p 403.

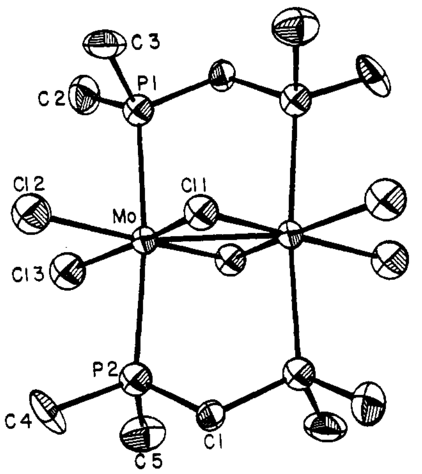

**Figure 1.** The $Mo_2Cl_6(dmpm)_2$ molecule with the atoms in one asymmetric unit labeled. Atoms are represented by their thermal displacement ellipsoids drawn at the 50% level. The structures of $W_2Cl_6(dmpm)_2$ and $Re_2Cl_6(dmpm)_2$ are generally similar and are labeled in a corresponding manner.

**Table VI.** Principal Molecular Dimensions[a,b]

| | 1 | 2 | 3 | 4 |
|---|---|---|---|---|
| | | Distances (Å) | | |
| M-M′ | 2.7394 (5) | 2.6663 (4) | 2.691 (1) | 2.5807 (4) |
| M-Cl(1) | 2.392 (1) | 2.385 (2) | 2.405 (3) | 2.368 (2) |
| M-Cl(1)′ | 2.387 (1) | 2.385 (2) | 2.393 (3) | 2.370 (2) |
| M-Cl(2) | 2.430 (1) | 2.441 (2) | 2.412 (3) | 2.410 (2) |
| M-Cl(3) | 2.427 (1) | 2.437 (2) | 2.408 (4) | 2.407 (2) |
| M-P(1) | 2.551 (1) | 2.541 (2) | 2.561 (3) | 2.436 (2) |
| M-P(2) | 2.554 (1) | 2.527 (2) | 2.566 (3) | 2.438 (2) |
| | | Angles (deg) | | |
| M-Cl(1)-M′ | 69.95 (2) | 67.97 (5) | 68.23 (9) | 66.01 (5) |
| Cl(1)-M-Cl(1)′ | 110.05 (2) | 112.03 (6) | 111.77 (9) | 113.99 (7) |
| Cl(2)-M-Cl(3) | 84.70 (4) | 84.23 (7) | 84.1 (1) | 82.66 (8) |

[a] The atom labeling is defined in Figures 1 and 2. [b] Figures in parentheses are esd's occurring in the last significant figure.

structure of compound **1** showing the atom-labeling scheme. Compounds **2** and **4** can be adequately represented by the same drawing. All three reside on crystallographic centers of symmetry, and the atoms were similarly labeled. Figure 2 shows the molecule of compound **3** and its labeling scheme. Here again the molecule has a crystallographic inversion center.

For all compounds, key bond lengths and angles are collected in Table VI. Complete lists of molecular dimensions for each compound are available as supplementary material. Some general, expected trends are seen throughout the series. Because each molecule is rigorously centrosymmetric, the central $M_2(\mu\text{-}Cl)_2$ rhombus is planar. Therefore, the order of increasing M-Cl(1)-M′ angles is the order of decreasing Cl(1)-M-Cl(1)′ angles. Because of the large values (ca. 112°) of the Cl(1)-M-Cl(1)′ angles, the Cl(2)-M-Cl(3) angles are all well below 90°, namely around 83°.

## Discussion

The present work has led to three important conclusions:

(1) A change from dmpm to dppm may cause significant changes in all dimensions of the molecule, including the M-M bond length.

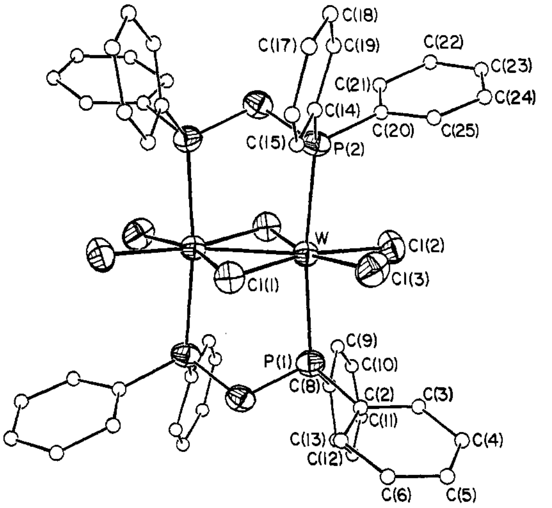

**Figure 2.** The $W_2Cl_6(dppm)_2$ molecule with the atoms in one asymmetric unit labeled. For atoms whose thermal displacement ellipsoids are shown, the contours are at the 50% level. The phenyl carbon atoms are represented by circles of arbitrary size.

(2) Homologous molecules with metal atoms from the second and third transition series may have appreciably different M-M bond lengths.

(3) Despite the above factors, which were not properly handled in the earlier work, the trends in M-M distances as a function of electronic configuration are the same as those previously observed and lead to the same conclusions concerning the order of filling of molecular orbitals.

Each of these points will now be discussed in detail.

**(1) $M_2Cl_6(dmpm)_2$ vs $M_2Cl_6(dppm)_2$ Structures.** Three such pairs (as opposed to none heretofore) are now available for comparison. Pertinent bond lengths are listed in Table VII. Bond length differences in each pair follow the same pattern for all three pairs. First, the M-P distances are, on average, 0.034 Å longer in the dppm compounds. This is to be expected because of the lower basicity of the phosphorus atoms in dppm. Second, the M-$Cl_t$ bonds are shorter by 0.020-0.032 Å in the dppm compounds. This could be regarded as a simple secondary effect of the weaker M-P donor bonding, in the sense that, with less electron density reaching the metal atoms from the phosphorus atoms, the metal atoms would retain a greater fractional positive charge and thus attract the chloride ligands more strongly.

The most important result of changing from dmpm to dppm is that the M-M bond lengths increase, by 0.050, 0.025, and 0.035 Å for the Mo, W, and Re compounds, respectively. There are also small increases in the M-$Cl_{br}$ distances, of 0.013, 0.014, and 0.021 Å, which may be regarded as secondary effects of the increases in the M-M distances. These increases in the M-M bond lengths may be attributed to the lower basicity of the dppm ligands, which results in there being greater positive charge on the metal atoms. This in turn causes some contraction in the metal d orbitals so that they overlap less well across the M-M gap and thus produce a weaker—and longer—M-M bond. An effect of this nature had been expected, but its magnitude was not predictable.

**(2) Molybdenum vs Tungsten Structures.** In our previous work we compared the $Nb_2Cl_6(dmpm)_2$ and $Ta_2Cl_6(dmpm)_2$ molecules and found only a small difference between the M-M bond lengths,

**Table VII.** Comparison of Bond Lengths (Å)[a] in Pairs of $M_2Cl_6(dmpm)_2$ and $M_2Cl_6(dppm)_2$ Compounds

| | M = Mo | | M = W | | M = Re | |
|---|---|---|---|---|---|---|
| bond | dmpm | dppm | dmpm | dppm | dmpm | dppm |
| M-M | 2.7394 (5) | 2.789 (1) | 2.6663 (4) | 2.691 (1) | 2.5807 (4) | 2.616 (1) |
| M-$Cl_{br}$(av) | 2.390 (3) | 2.403 (1) | 2.385 (0) | 2.399 (6) | 2.369 (1) | 2.390 (2) |
| M-$Cl_t$(av) | 2.428 (2) | 2.396 (4) | 2.439 (2) | 2.410 (2) | 2.408 (2) | 2.388 (3) |
| M-P(av) | 2.552 (2) | 2.586 (2) | 2.534 (7) | 2.564 (3) | 2.437 (1) | 2.475 (4) |

[a] Average values are arithmetic means with the mean deviation from the mean (in 0.001 unit) given in parentheses.

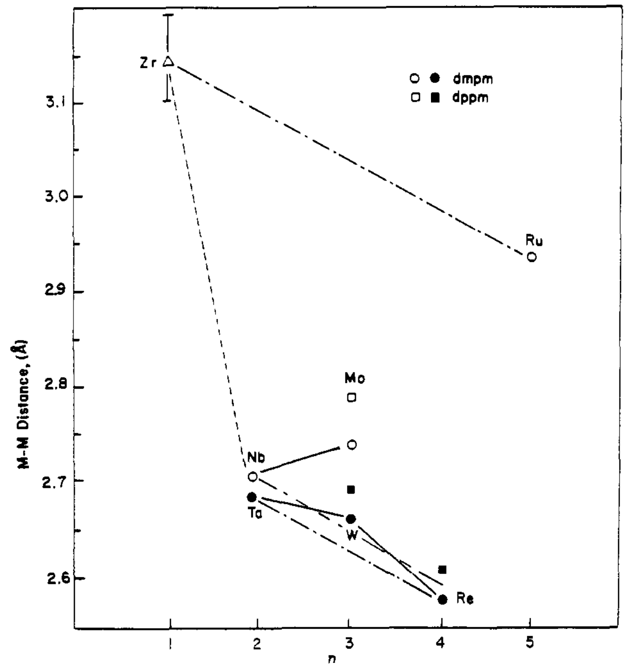

**Figure 3.** M–M distances in nine compounds of type I vs the number of electron pairs available for M–M interactions. Solid points are for third-row metals; open points are for second-row metals.

namely, 0.019 (4) Å. This was taken as an indication that in general it would be acceptable to employ a mixed set of compounds, some containing second-row and others containing third-row transition metals. The results that we now have with pairs of Mo and W compounds show that the result obtained with the Nb/Ta pair was not typical and that the differences can be larger. The differences ($d_{\text{Mo-Mo}} - d_{\text{W-W}}$) obtained for the $M_2Cl_6(dmpm)_2$ and $M_2Cl_6(dppm)_2$ pairs are 0.0731 (7) and 0.098 (2) Å, respectively. These differences are large enough that indiscriminate mixing of data from the two series of compounds is not permissible. We have attempted (and are continuing to try) to obtain technetium compounds for comparison with the rhenium ones, but thus far we have had no success.

The cause of the rather large Mo/W differences, ca. 0.08 Å, is not easily identified. The accepted metal atom radii[8] do not differ by nearly enough to account for it (only by 0.008 Å), nor do the various metal to ligand distances in these same compounds show comparable differences. Indeed, the corresponding pairs of $M-Cl_t$ distances are actually *larger* for the W compounds, although the M–P distances are roughly 0.02 Å shorter for the W compounds. It is our view that we are observing here a manifestation of an intrinsically greater tendency of the heavier d-block transition metals to engage in M–M bonding. A general trend in this direction has long been recognized and is exemplified, for example, by the existence in $[M_2X_9]^{3-}$ ions of no bond for Cr, a moderate bonding interaction for Mo, and a strong, short bond for W.

**(3) Molecular Orbital Interpretation.** With the additional data now available, bearing in mind the caveats thereby raised with respect to certain assumptions made in the earlier study,[1] we now take a fresh look at the question of how the M–M bond lengths change as we change the number of electron pairs ($n$) to be placed in the molecular orbitals having $\sigma$, $\pi$, $\delta$, $\delta^*$, $\pi^*$, and $\sigma^*$ character with respect to M–M bonding. Figure 3 will be helpful in discussing this question. It shows the M–M distances for all of the nine compounds of type I plotted vs the number of electron pairs, $n$.

Ideally, only a series of compounds all represented by exactly the same type of symbol (● or □ etc.) can safely be employed, and it is clear that we still do not have such a series extending over the entire range of $n$. However, we do now have the critical region, from 2 to 4, so covered by the three $M_2Cl_6(dmpm)_2$ compounds of Ta, W, and Re. It is these three points that provide the crux of the argument that proceeds as follows.

We note that the Ta and Re compounds have the same M–M bond order (2) regardless of the order in which the $\delta$ and $\delta^*$ orbitals are filled because for the Ta compound neither is filled and for the Re compound both are filled. The difference in their bond lengths, 0.111 (2) Å, should represent the difference in metal radii (×2). That this is so is strongly supported by the fact that, from Pauling's estimates of metal atomic radii,[8] the difference would be calculated to be 0.120 Å.

The question of whether the W compound should be assigned a $\sigma^2\pi^2\delta^2$ or a $\sigma^2\pi^2\delta^{*2}$ configuration is then to be decided by whether the observed W–W distance lies below or above the –·– line connecting the points for the Ta and Re compounds. Clearly, it lies above and the conclusion is that we have a $\sigma^2\pi^2\delta^{*2}$ configuration. This, of course, is the same conclusion previously reached on what are now seen to have been less rigorous grounds. Similarly, if we estimate the as yet unknown Tc–Tc distance in the $Tc_2Cl_6(dmpm)_2$ molecule by extrapolating from the Nb–Nb distance on the basis of the Pauling metal atomic radii, we can draw the other –·– line shown originating at the point for $Nb_2Cl_6(dmpm)_2$. Again, the point for the compound with $n = 3$ is above it (in this case by a great deal), leading very clearly to the $\sigma^2\pi^2\delta^{*2}$ assignment.

**(4) Other Observations.** While we have so far been unable to make a zirconium compound of type I, we have made and structurally characterized a number of other $Zr_2Cl_6(PR_3)_4$ compounds and found that all of them have Zr–Zr distances of 3.15 ± 0.05 Å. Such a point represented by a triangle is shown in Figure 3, as an estimate of where the Zr–Zr distance for $Zr_2Cl_6(dmpm)_2$ would fall. It is interesting that by extrapolating back from the known M–M distance in the $Ru_2Cl_6(dmpm)_2$ compound (which has a net $\sigma$ single bond based on the $\sigma^2\pi^2(\delta\delta^*)^4\pi^{*2}$ configuration) along a line parallel to that used to connect the points for the analogous Nb and Tc compounds, we come to the same position marked by the triangle. The internal consistency of the relationships is thus supported.

**Acknowledgment.** We are grateful to the National Science Foundation for support.

**Registry No.** **1**, 110796-23-1; **2**, 110796-25-3; **3**, 106297-42-1; **4**, 110796-26-4; $Mo_2Cl_4(dmpm)_2$, 104091-99-8; $W_2Cl_4(dppm)_2$, 110796-27-5; $W_2(SPh)Cl_5(dppm)_2$, 110825-36-0; $W_2Cl_4[P(n\text{-}Bu)_3]_4$, 73133-23-0; $(n\text{-}Bu_4N)_2Re_2Cl_8$, 14023-10-0; $CH_2Cl_2$, 75-09-2; PhSSPh, 882-33-7; W, 7440-33-7; Mo, 7439-98-7; Re, 7440-15-5; chlorine, 7782-50-5.

**Supplementary Material Available:** For the crystal structures of $Mo_2Cl_6(dmpm)_2$, $W_2Cl_6(dmpm)_2$, $W_2Cl_6(dppm)_2$, and $Re_2Cl_6(dmpm)_2$ full lists of bond distances, bond angles, and anisotropic displacement parameters (11 pages); lists of observed and calculated structure factors (41 pages). Ordering information is given on any current masthead page.